

ARTICLES

The Effect of Low-Temperature Dynamics of the Dimethylammonium Group in $[(\text{CH}_3)_2\text{NH}_2]_3\text{Sb}_2\text{Cl}_9$ on Proton Spin–Lattice Relaxation and Narrowing of the Proton NMR Line**L. Latanowicz,^{*,†} W. Medycki,[‡] and R. Jakubas[§]**

Department of Biophysics, Institute of Biotechnology and Environmental Sciences, University of Zielona Gora, Monte Cassino 21 B, 65-561 Zielona Gora, Poland, Institute of Molecular Physics, PAN, Smoluchowskiego 17, 60-179, Poland, and Faculty of Chemistry, University of Wrocław, 50-383 Wrocław, Poland

Received: October 28, 2004; In Final Form: February 4, 2005

This paper reports the temperature dependence of the relaxation time T_1 (55.2 and 90 MHz) and the second moment of the NMR line for protons in a polycrystalline sample of $[\text{NH}_2(\text{CH}_3)_2]_3\text{Sb}_2\text{Cl}_9$ (DMACA). The fundamental aspects of molecular dynamics from quantum tunneling at low temperatures to thermally activated reorientation at elevated temperatures have been studied. The experimentally observed spin–lattice relaxation rate is a consequence of dipolar interactions between the spin pairs inside the methyl group ($1/T_{1\text{AE}}$ contribution) as well as the spins belonging to neighboring methyl groups and pairs, methyl spin–outer methyl spin ($1/T_{1\text{EE}}$ contribution). These contributions are considered separately. Two methyl groups in the dimethylammonium (DMA) cations are dynamically inequivalent. The values of the tunnel splitting of separate methyl groups are obtained from the T_1 (55.2 MHz) experiment. The tunneling dynamics taking place below the characteristic temperatures 74 and 42 K for separate methyl groups are discussed in terms of the Schrödinger equation. These temperatures point to the one at which thermal energy $C_p T$ and potential barrier take the same value. It is established that the second moment of the proton NMR line below 74 K up to liquid helium temperature is much lower than the rigid lattice value, which is due to a tunneling stochastic process of the methyl groups.

1. Introduction

The methyl group is the ideal system for studying the fundamental aspects of molecular motion in solids because it undergoes rotational tunneling as well as thermally activated reorientation. The experimentally obtained temperature dependencies of the spin–lattice relaxation time, T_1 , and the second moment of the NMR line, M_2 , for methyl bearing solids are considerably different from those recorded for other solids.

The first to investigate the mechanism of CH_3 group reorientation in solids by NMR were Gutowsky and Pake,¹ Andrew,² and Powles and Gutowsky.^{3,4} Later,^{5,6} the mechanism of the CH_3 group rotational tunneling was considered in some detail. For a number of methyl-bearing solids the relaxation time T_1 at the minimum, observed even at high temperatures, is longer than that predicted on the basis of the known theories relating the T_1 relaxation with the classical C_3 rotation of the methyl group.^{6–12} This property is due to large tunnel splitting of the spin levels in a magnetic field for the methyl group protons. The tunnel splitting ω_T is imposed by the symmetry of the methyl group.¹³

* Address correspondence to this author. E-mail: jlat@amu.edu.pl.
Phone: 048 61 6639787. Fax: 048 61 8798202.

[†] University of Zielona Gora.

[‡] Institute of Molecular Physics.

[§] University of Wrocław.

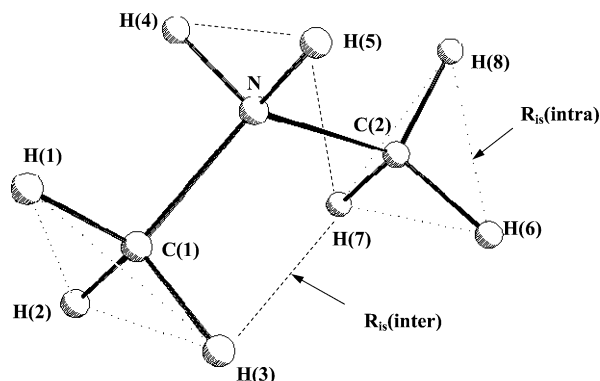


Figure 1. The structure of the $(\text{CH}_3)_2\text{NH}_2^+$ (DMA) cation. The distances $R_{is}(\text{intra})$ and exemplary $R_{is}(\text{inter})$ are marked with dotted and dashed lines, respectively.

The alternative theory explaining the long T_1 at the minimum has been proposed in ref 14. The theory demonstrates that the torsional oscillations of methyl groups, occurring at frequencies too high to influence spin relaxation rates directly, partially average the Hamiltonian for the magnetic dipole–dipole interactions between the nuclei. The efficiency of nuclear relaxation resulting from hindered rotation is thus reduced. The two maximums of relaxation rates both being inversely proportional to the Larmor frequency have been explained for the methyl group attached to a benzene ring in the stochastic model proposed in refs 15 and 16.

In terms of the relaxation theory assuming the classical motion only it is impossible to correlate the second moment (M_2) results with the results of the relaxation time T_1 measurements. The temperature dependence of the second moment may not show any changes even when considering the range from the liquid helium temperature, and its value can be a few times lower than that calculated for the rigid structure. Andrew et al.¹⁷ found that even at liquid helium temperatures the second moment of the NMR line of trimethylbenzene did not reach the value predicted for the rigid molecule. Eades et al.^{18,19} reported that NMR spectra of a number of compounds containing methyl groups measured at liquid helium temperatures are often narrow, indicating rotational motion of the methyl groups. Allen²⁰ gave the first simple model to explain the reduced value of the proton second moment of the NMR line (M_2) in methyl-bearing compounds at low temperatures. The spectral densities of complex motion derived in the ref 21 have been used in this work to explain the second moment of the proton NMR line much being lower than the rigid lattice value in the material studied.

The spin level system of methyl protons significantly different from that predicted for two uncoupled spins.²² In the system of three spins belonging to the methyl group, the transitions between the levels corresponding to the resonance frequencies ω_1 and $2\omega_1$ are forbidden.¹³ As the theory of relaxation has been propounded for a two-spin system, the occurrence of the tunnel splitting of the methyl group demands differentiation of two relaxation channels. The relaxation in the system of spin pairs $R_{is}(\text{intra})$ (dotted lines in Figure 1) belonging to the methyl group, the so-called $(1/T_{1AE})$ relaxation, is driven by the transitions between the nuclear spin levels corresponding to the frequencies $(\omega_T \pm \omega_1)$, $(\omega_T \pm 2\omega_1)$ and the relaxation in the systems of the other spin pairs in the molecule distanced by $R_{is}(\text{inter})$ (dashed lines in Figure 1), the so-called $(1/T_{1EE})$ relaxation, is driven by the transitions corresponding to the

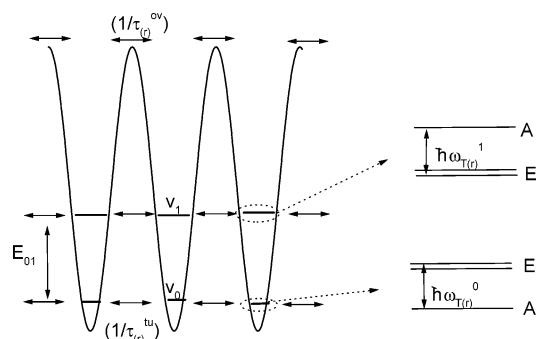


Figure 2. Schematic representation of motion in a periodic triple potential well. The symbols $(1/\tau^{ov})$ and $(1/\tau^u)$ are the rate constants of classical jumps across the barrier and tunneling jumps through the barrier. The two lowest torsional energy levels v_0 and v_1 , distanced by E_{01} , exhibit a tunnel splitting $h\omega_T$ into the levels with the symmetry A and E .

frequencies ω_1 and $2\omega_1$. Such an approach to the spin–lattice relaxation of the methyl bearing solid has been proposed by Haupt.¹³

The methyl group undergoes hindered rotation in a triple potential well (Figure 2). This motion is complex, consisting of hopping over the barrier (hopping across the barrier, classical motion, classical C_3 rotation) and hopping through the barrier (incoherent tunneling, quantum mechanical tunneling). Because of these compound motions the orientation and the values of $R_{is}(\text{intra})$ and $R_{is}(\text{inter})$ vectors are random functions of time. The theory of classical C_3 rotation of the methyl group, which is a dominant mechanism of relaxation at high temperatures, is well-known.²³ This paper reports the occurrence of the tunneling jumps of the methyl protons in the $(\text{CH}_3)_2\text{NH}_2^+$ (DMA) cation as the dominant mechanism of spin–lattice relaxation in the low-temperature regime. Moreover, in this paper it is shown that although the tunnel splitting ω_T takes place also at high temperatures, the spectral densities related to the tunneling jumps are zero at high temperatures. The presence of the tunneling process is predicted by the Schrödinger equation for the energies of particles lower than the potential barrier. The tunneling jumps of proton through the barrier should cease above the temperature at which the thermal energy of the molecule is higher than the potential barrier for the hindered rotation of the methyl group. The damping of the correlation function related to the incoherent tunneling at high temperatures has been established for the proton transfer in the hydrogen bond.^{24,25}

The conclusions drawn on the basis of the spectral densities of particular motions calculated in refs 24–26 contradict the generally assumed scheme implying that the classical motion takes place only at high temperatures.⁷ The probability of classical jumps is higher than zero in the whole temperature regime up to 0 K, while that of tunneling jumps is higher than zero only at low temperatures.

DMACA in the paraelectric phase crystallizes in a monoclinic symmetry, space group $P2_1/c$ ($a = 14.074(2) \text{ \AA}$, $b = 9.048(2) \text{ \AA}$, $c = 9.692(3) \text{ \AA}$, $\beta = 95.56(2)^\circ$, $Z = 2$). The crystals are built of two-dimensional layers of corner sharing halogen octahedra.²⁷ The dimethylammonium (DMA) cations situated in cavities between the octahedra possess substantial freedom for reorientations. The ionic salts containing the DMA cations are known to undergo structural phase transitions. The phase transition at 242 K leads to the ferroelectric phase with a polar symmetry m (space group Pc).²⁷ From the dielectric studies of DMACA it appears that the ferroelectric phase transition is of the order–disorder type. The mechanism of this phase transition is associated with changes in the dynamics of the DMA

cations.^{28–33} The high-temperature dynamics of the alkylammonium cation has been studied, both below and above the transition by NMR spectroscopy.^{34–36} This paper presents proton NMR studies of DMA cation dynamics below the liquid nitrogen temperature.

2. Theory

Proton Spin–Lattice Relaxation. The theory of magnetic nuclear relaxation for methyl bearing solids must distinguish between the spin pairs belonging to the same methyl group, R_{is} (intra), and spin pairs made of one spin belonging to the methyl group considered while the other is outside it (it can belong to another molecular group), R_{is} (inter) (Figure 1). This distinction is necessary because the splitting ω_T of the torsional ground state of the methyl group is usually superimposed on the three spin level splitting ω_I in a magnetic field (Figure 2), while the theory of relaxation concerns two-spin systems. For the spin pair at the distance R_{is} (inter), the spin–lattice relaxation can be realized through transitions forced by a fluctuating local field of the frequencies ω_I and $2\omega_I$, which are forbidden for the spin pairs at the distance R_{is} (intra). For the latter spin pairs the allowed transitions are $(\omega_T \pm \omega_I)$ and $(\omega_T \pm 2\omega_I)$. Hence, the total relaxation rate of the eight protons in the DMA cation with two methyl groups (I) and (II), denoted as in Figure 1, is a sum of two relaxation rates:

$$\left(\frac{1}{T_1}\right)_{vx} = \left(\frac{1}{T_{1AE}}\right)_{vx} + \left(\frac{1}{T_{1EE}}\right)_{vx} \quad (1)$$

where

$$\left(\frac{1}{T_{1AE}}\right)_{vx} = \frac{1}{8} \sum_{i=1}^3 \sum_{s=1}^3 \left(\frac{1}{T_{1AE}^{is}(\text{I})}\right)_{vx} + \frac{1}{8} \sum_{i=6}^8 \sum_{s=6}^8 \left(\frac{1}{T_{1AE}^{is}(\text{II})}\right)_{vx} \quad (2)$$

$$\left(\frac{1}{T_{1EE}}\right)_{vx} = \frac{1}{8} \sum_{i=4}^8 \sum_{s=1}^3 \left(\frac{1}{T_{1EE}^{is}(\text{I})}\right)_{vx} + \frac{1}{8} \sum_{i=1}^5 \sum_{s=6}^8 \left(\frac{1}{T_{1EE}^{is}(\text{II})}\right)_{vx} \quad (3)$$

The indices (I) and (II) mean that the motion parameters refer to the methyl group (I) or (II). The symbol $(1/T_{1AE}^{is})$ refers to the spin–lattice relaxation of two nuclear spins at the distance R_{is} (intra), while $(1/T_{1EE}^{is})$ refers to the relaxation in the system of two spins at the distance R_{is} (inter). The indices vx, where $x = 0, 1, 2, \dots$, were introduced to take into account the fact that the molecules can be distributed on the torsion levels according to the Boltzmann distribution. The problem is discussed in detail in the paper²⁶ showing that for proton relaxation it is enough to consider the two ground and first excited torsional levels. Therefore, the total relaxation rate is

$$\left(\frac{1}{T_1}\right) = n_{v0} \left(\frac{1}{T_1}\right)_{v0} + n_{v1} \left(\frac{1}{T_1}\right)_{v1} \quad (4)$$

where n_{v0} and n_{v1} are the fractions of molecules on the vx = v0 and vx = v1 levels.

Particular contributions to the total relaxation rate $(1/T_1)$ are functions of spectral densities depending on the model of motion. According to the model presented in ref 26, the spectral densities depend on the two different correlation times: (1) the correlation time of jumps over the barrier (classical motion), which fulfils the Arrhenius dependence,

$$\tau_{(r)}^{ov} = \tau_{0(r)}^{ov} \exp(E_{(r)}^{ov}/RT) \quad (5)$$

where $E_{(r)}^{ov}$ is the molar potential barrier height and $r = \text{I, II}$ labels the methyl group, and (2) the correlation time of tunnel jumps expressed by the equation which follows from the Schrödinger equation,³⁷

$$\tau_{(r)}^{tu} = \tau_{0(r)}^{tu} \exp[B\sqrt{(E_{(r)}^{ov} - C_p T)}] \quad (6)$$

where

$$B = \frac{2L}{\hbar} \sqrt{\frac{2m}{N_{AV}}} \quad (7)$$

The value of B in eq 7 depends on the mass “ m ” of the tunneling particle and on the width of the potential barrier “ L ”. $C_p T$, where C_p is the molar specific heat, T is the temperature in the Kelvin scale, is the thermal energy and $E_{(r)}^{ov}$ is the potential energy barrier of the Avogadro number of particles.

Therefore, as the BPP theory predicted³⁸

$$\frac{1}{T_{1EE}^{is}} = \frac{9}{8} [J_{is}^1(\omega_I) + J_{is}^2(2\omega_I)] \quad (8)$$

and according to the Haupt theory¹³

$$\frac{1}{T_{1AE}^{is}} = \frac{9}{16} [J_{is}^1(\omega_T + \omega_I) + J_{is}^1(\omega_T - \omega_I) + J_{is}^2(\omega_T + 2\omega_I) + J_{is}^2(\omega_T - 2\omega_I)] \quad (9)$$

where the spectral densities

$$J_{is}^m(\omega) = \int_{-\infty}^{\infty} \langle F_{is}^m(t) F_{is}^{m*}(t + \tau) \rangle \exp(-i\omega\tau) d\tau \quad (10)$$

are Fourier transforms of the autocorrelation functions of the random functions of the dipolar perturbation Hamiltonian. These random functions are

$$F_{is}^1(t) = d_c^{is}(t) \sin\vartheta_{is}(t) \cos\vartheta_{is}(t) \exp(i\varphi_{is}(t)) \quad (11)$$

$$F_{is}^2(t) = d_c^{is}(t) \sin^2\vartheta_{is}(t) \exp(i2\varphi_{is}(t)) \quad (12)$$

Since spins (i) and (s) belong to the molecule undergoing stochastic motions, the coordinates $(R_{is}, v_{is}, \varphi_{is})$ are random functions of time. R_{is} is the distance between spins (i) and (s). v_{is} and φ_{is} are the polar and azimuth angles, respectively, describing the orientation of the internuclear vector in the laboratory frame with the z axis in the direction of the external magnetic field B_0 . $d_c^{is}(t) = \gamma_i \gamma_s \hbar R_{is}^{-3}(t)$ is the dipolar coupling constant. As in the polycrystalline material particular spin pairs can assume arbitrary angles v_{is} and φ_{is} , the calculations of $J_{is}^m(\omega)$ were performed for the mean values $[\sin v_{is} \cos v_{is} \exp(i\varphi_{is})]^2 = 2/15$ ($S^1 = 2/15$) and $[\sin^2 v_{is} \exp(2i\varphi_{is})]^2 = 8/15$ ($S^2 = 8/15$). Therefore, after spatial averaging the total spectral density of complex motion consisting of the classical motion and incoherent tunneling has been derived in ref 26:

$$J_{is}^m(\omega) = S^m [d_c^{is}(A)]^{-2} \left[C_1^{is} C_2^{is} \frac{2\tau_{(r)}^{tu}}{1 + (\omega\tau_{(r)}^{tu})^2} + C_1^{is} C_2^{is} \frac{2\tau_{(r)}^{ov}}{1 + (\omega\tau_{(r)}^{ov})^2} + (C_2^{is})^2 \frac{2\tau_{(r)}^{ovu}}{1 + (\omega\tau_{(r)}^{ovu})^2} \right] \quad (13)$$

$S^m = 2/15, 8/15$ for $m = 1, 2$ and

$$C_1^{is} = \frac{1}{9}[d_c^{is}(A)^2 + d_c^{is}(B)^2 + d_c^{is}(C)^2 + d_c^{is}(A)d_c^{is}(B)(3 \cos^2 \Theta_{AB}^{is} - 1) + d_c^{is}(A)d_c^{is}(C)(3 \cos^2 \Theta_{AC}^{is} - 1) + d_c^{is}(B)d_c^{is}(C)(3 \cos^2 \Theta_{BC}^{is} - 1)] \quad (14)$$

$$C_2^{is} = \frac{1}{9}[2d_c^{is}(A)^2 + 2d_c^{is}(B)^2 + 2d_c^{is}(C)^2 - d_c^{is}(A)d_c^{is}(B)(3 \cos^2 \Theta_{AB}^{is} - 1) - d_c^{is}(A)d_c^{is}(C)(3 \cos^2 \Theta_{AC}^{is} - 1) - d_c^{is}(B)d_c^{is}(C)(3 \cos^2 \Theta_{BC}^{is} - 1)] \quad (15)$$

$$\frac{1}{\tau_{(r)}^{ovm}} = \frac{1}{\tau_{(r)}^{ov}} + \frac{1}{\tau_{(r)}^{u}} \quad (16)$$

where $d_c^{is}(A) = \gamma_i \gamma_s \hbar R_{is}^{-3}(A)$, $d_c^{is}(B) = \gamma_i \gamma_s \hbar R_{is}^{-3}(B)$, $d_c^{is}(C) = \gamma_i \gamma_s \hbar R_{is}^{-3}(C)$ are the particular dipolar coupling constant values. $R_{is}(A)$, $R_{is}(B)$, and $R_{is}(C)$ are the distances between the spins “i” and “s” at three equilibrium positions in a triple potential minimum during the hindered rotation C_3 of a given methyl group. If the spins “i” and “s” belong to the same methyl groups, the distance between them does not change, so $R_{is}(A) = R_{is}(B) = R_{is}(C)$, but if they belong to different methyl groups, or spin “i” belongs to the rotating methyl group and spin “s” to another chemically inequivalent group then $R_{is}(A) \neq R_{is}(B) \neq R_{is}(C)$. The angles Θ_{AB}^{is} , Θ_{AC}^{is} , Θ_{BC}^{is} are those made by $R_{is}(A)$, $R_{is}(B)$, $R_{is}(C)$ (Figure 1).

The condition if $C_p T > E_{(r)}^{ov}$ then

$$J_{is}^m(\omega) = S^m C_2^{is} \frac{2\tau_{(r)}^{ov}}{1 + (\omega\tau_{(r)}^{ov})^2} \quad (17)$$

confirms, following from the Schrödinger equation, the cessation of the tunneling motion ($\tau_{(r)}^{u} \rightarrow \infty$) at the characteristic temperature T_{tun} at which $C_p T_{\text{tun}} = E_{(r)}^{ov}$. The spectral densities are governed by the classical motion only at temperatures $T > T_{\text{tun}}$. Below temperature T_{tun} the probability of tunneling stochastic process becomes higher than zero (eq 6).

The classical motion also can be complex (for example, consisting of hindered rotation in triple potential and isotropic rotation). Then the next T_1 minima at higher temperatures are expected.^{39,40}

Second Moment of the Proton NMR Line. The basic equation for the dipolar second moment, M_2 , of a dipolar NMR line was derived by Van Vleck⁴¹ for two identical nuclei in the presence of a motion for which $\tau_c \ll 1/(\gamma\sqrt{M_{2is}^{\text{rigid}}})$, where M_{2is}^{rigid} is the rigid lattice second moment in magnetic field units,

$$M_{2is}^{\text{motion}} = \frac{3}{4}\gamma_i^{-2}I(I+1)\langle [F_{is}^0(t)]^2 \rangle \quad (18)$$

where

$$F_{is}^0(t) = d_c^{is}(t)[3 \cos^2 \vartheta_{is}(t) - 1] \quad (19)$$

is a random function in the dipolar perturbation Hamiltonian.

When N is the number of interacting nuclei then M_{2is}^{motion} is given by the averaged sum of the N dipolar interactions:

$$M_2^{\text{motion}} = \frac{3}{4}\gamma_i^{-2}I(I+1)N^{-1}\sum_{i=1}^N\sum_{s=1}^N\langle [F_{is}^0(t)]^2 \rangle \quad (20)$$

The maximum reduction in the second moment occurs at temperatures at which all the molecules reorient fast enough to reduce the line broadening. As proposed by Powles and Gutowsky,⁴ the stochastic nature of the motion permits the application of the correlation function method. If the correlation function of a given reorientation is known, the appropriate averages for the partial averaging of $\langle [F_{is}^0(t)]^2 \rangle$ are of the form

$$\langle [F_{is}^0(t)]^2 \rangle = \int_{-\delta\nu}^{\delta\nu} J_{is}^0(\nu) d\nu \quad (21)$$

where $\delta\nu$ is the line width, $\omega = 2\pi\nu = \gamma\sqrt{M_2}$, and $J_{is}^0(\omega)$ is the spectral density of the correlation function of the random function $F_{is}^0(t)$.

Therefore, as proposed by Powles and Gutowsky the equation for M_2 extended over the whole temperature regime is of the form

$$M_2 = \frac{3}{4}\gamma_i^{-2}I(I+1)N^{-1}\sum_{i=1}^N\sum_{s=1}^N\int_{-\delta\nu}^{\delta\nu} J_{is}^0(\nu) d\nu \quad (22)$$

The fractions n_{v0} and n_{v1} molecules distributed in two vibrational levels contribute to the second moment of the NMR line. Therefore, the total value of the second moment equals

$$M_2 = n_{v0}(M_2)_{v0} + n_{v1}(M_2)_{v1} \quad (23)$$

where n_{v0} and n_{v1} are the fractions of molecules at the ground and excited rotational levels. As we are going to consider the second moment reductions taking place at temperatures below the liquid nitrogen one, in eq 23 the contribution of $n_{v1}(M_2)_{v1}$ can be neglected because $n_{v0} \approx 1$ in this range. Thus, $M_2 \approx (M_2)_{v0}$.

Calculations of proton spin–lattice relaxation time as well as the proton second moment of the NMR line require the knowledge of the spectral densities of the expected motion of the spin system.

The three proton NMR lines at the frequencies ω_I , $(\omega_I + \omega_T)$, and $(\omega_I - \omega_T)$ are observed at liquid helium temperatures for methyl bearing compounds.⁷ The lines $(\omega_I \pm \omega_T)$ are distanced from the central line ω_I and usually are beyond the range of the central line measurement. The temperature dependencies of the second moment have to be considered separately for each line. Assuming that the dipolar interactions are additive, the total second moment of the line should include a sum of dipolar interactions over all spin pairs at the distances $R_{is}(\text{inter})$ as well as $R_{is}(\text{intra})$.

The total value of the second moment should include the dipole–dipole interactions of all spin pairs in the molecule. The contribution from two spins belonging to the NH_2 remains constant because no motion modulates the dipolar interaction of the protons within the NH_2 group. The other dipole–dipole interactions in the molecule are modulated by the motion of two methyl groups. Therefore, the total value of the second moment equals

$$M_2 = \frac{1}{8}\left[\sum_{i=1}^3\sum_{s=1}^8M_{2(i)}^{is} + \sum_{i=6}^8\sum_{s=1}^8M_{2(\text{II})}^{is} + \sum_{i=4}^5\sum_{s=1}^5M_{2(\text{I})}^{is} + \sum_{i=4}^5\sum_{s=6}^8M_{2(\text{II})}^{is}\right] \quad (24)$$

where

$$M_{2(r)}^{is} = \frac{9}{20\gamma^2} d_c^{is}(A)^{-2} [(C_1^{is})^2 + C_1^{is} C_2^{is} \frac{2}{\pi} \tan^{-1}(\gamma_i \tau_{(r)}^{ov} \sqrt{M_{2(r)}^{is}}) + C_1^{is} C_2^{is} \frac{2}{\pi} \tan^{-1}(\gamma_i \tau_{(r)}^{tu} \sqrt{M_{2(r)}^{is}}) + (C_2^{is})^2 \frac{2}{\pi} \tan^{-1}(\gamma_i \tau_{(r)}^{ovtu} \sqrt{M_{2(r)}^{is}})] \quad (25)$$

where C_1^{is} , C_2^{is} are given in eqs 14 and 15, and $\tau_{(r)}^{ov}$, $\tau_{(r)}^{tu}$, $\tau_{(r)}^{ovtu}$ are given in eqs 5, 6, and 16.

The reductions of the second moment should be observed when the rates of particular motions ($1/\tau_{(r)}^{tu}$), ($1/\tau_{(r)}^{ov}$) become comparable to the values of line widths on the frequency scale. The tunneling jumps in separate methyl groups reduce M_2 . This should happen at the temperatures at which the reorientation frequency meets the condition $(1/\tau_{(r)}^{tu}) \approx \gamma\sqrt{M_{2(r)}^{is}}$. Such a temperature regime is near 0 K. With temperature increasing, when the tunneling motion ceases the line should undergo broadening followed by narrowing at higher temperatures due to increasing classical motion. The two reductions which are due to classical dynamics of separate methyl groups are expected for proton M_2 of DMACA. The reductions should take place when $(1/\tau_{(r)}^{ov}) \approx \gamma\sqrt{M_{2(r)}^{is}}$. The classical motion of R_{is} can be complex (for example, the classical hindered rotation in a triple potential and isotropic rotation). Then the next reductions of M_2 are expected at higher temperatures. The corresponding equations for the temperature dependences of spectral density of complex motion derived in refs 39, 40, 42, and 43 may be applied to such a case.

3. Experimental Section

[(CH₃)₂NH₂]₃Sb₂Cl (DMACA) were precipitated from the stoichiometric aqueous solution of Sb₂O₃ and [NH₂(CH₃)₂]Cl at a high excess of HCl and purified by slow recrystallization. The pulverized single crystals of DMACA were degassed under a pressure of 10⁻⁵ Torr and sealed under vacuum in glass ampules.

The proton spin–lattice relaxation (T_1) measurements at a Larmor frequency 55.2 and 90 MHz and second moment experiments were carried out with a SXP 4/100 Bruker pulsed NMR spectrometer. Proton T_1 relaxation times were measured employing the (180°– τ –90°) pulse (IR) sequence for times shorter than 1 s and by the conventional saturation-recovery (SR) sequence [(90°– τ_1 –90°)_{*n*}– τ –90°] where $n = 15$. Delay τ_1 was typically 4 ms. For all data reported, the magnetization was found to recover exponentially. The second moment of the ¹H NMR line was calculated from a solid echo signal. Solid echo sequence⁴⁴ (90_x°– τ –90_y°) (with $\tau = 17 \mu\text{s}$) avoids signal loss during the dead time.^{45,46} The normalized line shape of the solid echo spectrum is identical with that of the FID spectrum. Therefore the second moment can be determined on the basis of analysis of the solid echo shape.⁴⁶ The temperature of the sample was automatically controlled by means of a gas-flow CF1200 Oxford cryostat with an accuracy of about 1 K during each measurement.

4. Results and Discussion

Proton Spin–Lattice Relaxation Time. The spin–lattice relaxation times for the protons of [(CH₃)₂NH₂]₃Sb₂Cl₉ (DMACA) were measured at the frequency 55.2 MHz from the liquid helium temperature to the melting point, and at the frequency 90 MHz from the liquid nitrogen temperature up to the melting

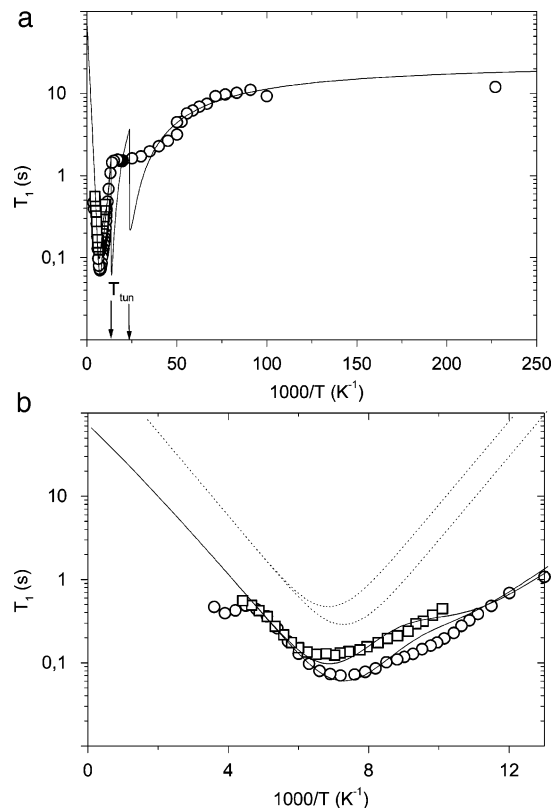


Figure 3. Temperature dependencies of the proton T_1 time (55.2 MHz, circles; 90 MHz, squares) and best fit curves (solid lines) for powdered samples of DMACA. The dotted lines in part b show the theoretical plots of $T_{1EE}(52.2 \text{ MHz})$ and $T_{1EE}(90 \text{ MHz})$ obtained from eq 3 and the motion parameters given in Table 2. Arrows show the temperatures $T_{\text{tun}(r)} = E_{(r)}^{ov}/C_p$ (74K and 42 K).

point. The value of T_1 due to classical motion depends on the resonance frequency ω_1 according to the known relation:

$$T_1^{\text{min}} = \frac{\omega_1}{1.425C} \quad (26)$$

where C is the relaxation constant depending on the model of motion.

Assuming that the methyl groups perform the correlated C_3 reorientation about the symmetry axis, the relaxation constant C becomes²³

$$C = \frac{n}{N} \frac{9}{20} \gamma^4 \hbar^2 R_{\text{CH}_3}^{-6} \quad (27)$$

where $n = 6$ is the number of protons in the methyl groups and $N = 8$ is the number of all protons in the molecule. $R_{\text{CH}_3} = 1.78 \text{ \AA}$ is the proton–proton distance in the methyl group. According to eq 27 we get $C = 60.4 \times 10^8 \text{ s}^{-2}$ and $T_1^{\text{min}}(90 \text{ MHz}) = 66 \text{ ms}$ and $T_1^{\text{min}}(55.2 \text{ MHz}) = 40 \text{ ms}$. The experimental T_1 times at the minima are about twice longer.

The character of the wide range temperature dependence of T_1 (Figure 3a) indicates that it cannot be interpreted in terms of the classical theory of molecular motion only. It seems that the only reasonable explanation of this course of $T_1(T)$ is based on the assumption of the complex motion of separate methyl groups. The complex motion consists of jumps over the barrier characterized by correlation time $\tau_{(r)}^{ov}$ and tunneling jumps characterized by the correlation time $\tau_{(r)}^{tu}$. The geometries of both compound motions are the same but the frequencies are different.

The high-temperature T_1 minimum is asymmetric, which suggests the presence of two minima close on the temperature scale. The slope of $\ln T_1(1000/T)$ dependence (Figure 3b) from the high-temperature side corresponds to the activation energy of 9.6 kJ/mol, while from the low-temperature side to 5.4 kJ/mol. The activation energies of this order characterize the classical motion. These values can be interpreted as corresponding to different potential barriers of the jumps over the barrier of two types of methyl groups. These dynamically inequivalent methyl groups can belong to one DMA cation or to two different cations belonging to two different molecules in the crystal cell. The distinction between both cases is rather impossible by the NMR relaxation method.

The significantly different potential barriers for the hindered rotation of separate methyl groups suggest that the respective tunnel splitting ω_T are different. This is also confirmed by fact that two minima close on the temperature scale do not take the same values. The analysis presented is performed assuming $n_{v0} = 1$ and $n_{v1} = 0$, which is correct for low temperatures and holds also for high temperatures, because the only difference between eq 4 and the following equation

$$\frac{1}{T_1} = \left(\frac{1}{T_1} \right)_{v0} \quad (28)$$

is the neglect of the fact that the value of the potential barrier is $(E_{(r)}^{ov} - E_{01})$ (Figure 2) for the fraction n_{v1} of the molecules. Thus, the potential barrier of the classical motion obtained from eq 28 is the average value of the potential barrier for molecules distributed between the $v0$ and $v1$ levels.

In the range of intermediate temperatures, the increase in T_1 at a rate of 5.4 kJ/mol breaks and the $\ln T_1(1000/T)$ dependence passes through two weakly marked minima of almost the same height, but the T_1 at these minima are a few times longer than at the high-temperature minimum. The intermediate temperature range covers $20 \text{ K}^{-1} < 1000/T < 60 \text{ K}^{-1}$. In the lowest temperatures the $\ln T_1(1000/T)$ dependence becomes flattened and linear down to liquid helium temperature (Figure 3a). The character of the intermediate and low temperature T_1 dependence follows from the characteristic temperature dependence of $\tau_{(r)}^{tu}$. The values of $\tau_{(r)}^{tu}$, which are almost constant at low temperatures, decrease significantly at the temperature regime below the $T_{\text{tun}(r)}$ temperature at which the tunneling motion ceases.

The results of the fit of eq 1 and eq 13 to the experimental relaxation times $T_1(55.2 \text{ MHz})$ and $T_1(90 \text{ MHz})$ are presented in Figure 3 by solid lines. The analysis of the temperature dependence of T_1 at high temperature range is additionally illustrated in Figure 3b showing, apart from the best-fitted curve, also the contribution of $T_{1\text{EE}}$ to the T_1 relaxation time. The values of $R_{\text{is}}(\text{A})$, $R_{\text{is}}(\text{B})$, $R_{\text{is}}(\text{C})$, $\Theta_{\text{is}}^{\text{AB}}$, $\Theta_{\text{is}}^{\text{BC}}$, and $\Theta_{\text{is}}^{\text{AC}}$ were not fitted but were taken from the available structural data.³⁰ The relaxation rate $(1/T_{1\text{EE}})$ depends on the fluctuations of the dipolar interactions of the spin pairs at the distances $R_{\text{is}}(\text{inter})$ (Figure 1). Because in the formulas for $(1/T_{1\text{EE}})$, the value of R_{is} occurs in the sixth power, the ensuing considerable changes in the distance cannot be neglected in analysis of the relaxation rate. According to Table 1, all $R_{\text{is}}(\text{inter})$ distances are from the range 2.2 to 2.9 Å. The values listed in Table 1 are calculated from the structural data.³⁰ The distances are much greater than R_{is} within the methyl group $R_{\text{is}}(\text{intra}) = 1.78 \text{ Å}$. The $(1/T_{1\text{EE}})$ contribution to the relaxation is much smaller than $(1/T_{1\text{AE}})$. Thus it can be concluded that the course of $T_1(T)$ in the whole temperature range is related to $(1/T_{1\text{AE}})$.

The best-fit parameters are given in Table 2. The values of the parameters influence the T_1 value in different temperature

TABLE 1: The Proton-Proton Distances (in Å) for the DMA Cation (Figure 1)

$R_{\text{H}(4)\text{H}(1)} = 2.19$	$R_{\text{H}(5)\text{H}(1)} = 2.19$	$R_{\text{H}(1)\text{H}(6)} = 4.08$	$R_{\text{H}(3)\text{H}(6)} = 3.68$
$R_{\text{H}(4)\text{H}(2)} = 2.82$	$R_{\text{H}(5)\text{H}(2)} = 2.23$	$R_{\text{H}(1)\text{H}(7)} = 3.75$	$R_{\text{H}(3)\text{H}(7)} = 2.60$
$R_{\text{H}(4)\text{H}(3)} = 2.23$	$R_{\text{H}(5)\text{H}(3)} = 2.82$	$R_{\text{H}(1)\text{H}(8)} = 3.74$	$R_{\text{H}(3)\text{H}(8)} = 3.15$
$R_{\text{H}(4)\text{H}(6)} = 2.36$	$R_{\text{H}(5)\text{H}(6)} = 2.36$	$R_{\text{H}(2)\text{H}(6)} = 3.68$	$R_{\text{H}(4)\text{H}(5)} = 1.67$
$R_{\text{H}(4)\text{H}(7)} = 2.40$	$R_{\text{H}(5)\text{H}(7)} = 2.96$	$R_{\text{H}(2)\text{H}(7)} = 3.15$	$R_{\text{H}(1)\text{H}(2)} = 1.78$
$R_{\text{H}(4)\text{H}(8)} = 2.95$	$R_{\text{H}(5)\text{H}(8)} = 2.40$	$R_{\text{H}(2)\text{H}(8)} = 2.60$	$R_{\text{H}(6)\text{H}(7)} = 1.78$

ranges. The values of $\tau_{0(r)}^{ov}$, $E_{(r)}^{ov}$, and $\omega_T(r)$ were obtained from the asymmetric high-temperature minimum, and $\tau_{0(r)}^{tu}$ and L were obtained from the low-temperature regime. The values of C_p and T_{tun} were estimated from the intermediate temperature regime ($20 \text{ K}^{-1} < 1000/T < 60 \text{ K}^{-1}$).

In conclusion, the course of $T_1(T)$ for DMACA reveals the presence of two dynamically inequivalent methyl groups with two different tunnel splittings. One of the tunnel splittings is small and cannot be precisely determined from T_1 experiment.²⁶ The other one ω_T is high enough ($2\pi \times 600 \text{ MHz}$) to be manifested as a significant increase in the corresponding value of T_1 minimum. The dominant mechanism of relaxation at the lowest temperatures is the tunneling because at this temperature range the spectral density of this type of motion takes the highest value.

Figure 4 presents the temperature dependence of the correlation times characterizing particular types of stochastic motion performed by the two methyl groups of the DMA cation denoted as (I) and (II). These motions are the classical hindered rotations (the lines $\tau_{(I)}^{ov}$, $\tau_{(II)}^{ov}$), tunneling jumps (the lines $\tau_{(I)}^{tu}$, $\tau_{(II)}^{tu}$). The lines were drawn using the best-fit parameters given in Table 2, and eqs 5 and 6. The points are the experimental correlation times.

Usually literature reports one uniform correlation time characterizing all stochastic processes in the molecule.^{7,11,47} Such a uniform correlation time does not follow the Arrhenius equation and diverts from it at the low-temperature range. The dependencies presented in Figure 4 differ from the temperature course of one uniform correlation time (Arrhenius diagram) known from the literature. We do not accept the idea of a uniform correlation time. The temperature dependencies of the $\tau_{(I)}^{ov}$, $\tau_{(II)}^{ov}$ times fulfill the Arrhenius equation in the whole temperature regime studied. The temperature dependencies of the $\tau_{(I)}^{tu}$, $\tau_{(II)}^{tu}$ can be plotted up to a certain characteristic temperature T_{tun} , where $C_p T_{\text{tun}} = E_{(r)}^{ov}$ only. Above this temperature the correlation functions of incoherent cannot be defined. Before the molecules reach the thermal energy $C_p T_{\text{tun}}$, the correlation times $\tau_{(I)}^{tu}$, $\tau_{(II)}^{tu}$ should undergo significant shortening.

Proton NMR Line Narrowing. The temperature dependence of the second moment of the proton NMR line for DMACA is shown in Figure 5. Even at the lowest temperatures the second moment does not reach the value determined for the rigid lattice. Usually, the second moment for the rigid lattice is calculated by assuming the Van Vleck theory,⁴¹ so by summing up the contributions from all dipolar interactions in the molecule, according to the formula

$$M_2^{\text{rig}} = \frac{9}{20} \gamma_i^2 \hbar^2 \sum_{n=1}^n \sum_{s=1}^n R_{\text{is}}^{-6} \quad (29)$$

where n is the number of all protons in the unit cell of the crystal.

For the rigid structure of $[(\text{CH}_3)_2\text{NH}_2]_3\text{Sb}_2\text{Cl}_9$ (DMACA) it is 31.9 G^2 . It is very interesting to note a very small difference between the rigid lattice second moment calculated for the

TABLE 2: The Motion Parameters Obtained for Methyl Groups in the DMA Cation from the T_1 Measurements

no. of methyl group	$\tau_{0(r)}^{ov}$, s	$\tau_{0(r)}^{tu}$, s	$E_{(r)}^{ov}$, kJ/mol	$T_{\text{tun}(r)}$, K	C_p , J (K/mol) ^{1/2}	L , nm	$\omega_{T(r)}$, MHz
$r = \text{I}$	$(4 \pm 0.5) \times 10^{-13}$	$(6 \pm 0.5) \times 10^{-10}$	9.6 ± 0.8	41 ± 5	130 ± 10	0.13 ± 0.01	$(0 \pm 2\pi(20))$
$r = \text{II}$	$(4 \pm 0.5) \times 10^{-13}$	$(6 \pm 0.5) \times 10^{-10}$	5.4 ± 0.8	73 ± 5	130 ± 10	0.13 ± 0.01	$2\pi(600 \pm 50)$

crystal cell and that calculated for the dimethylammonium group [(CH₃)₂NH₂⁺] which is 31.7 G². As follows from Figure 5, even at the lowest temperatures the second moment value is about twice smaller. According to the theory presented in Section 2, the second moment of the central ω_1 proton NMR line for the particular case of the DMACA molecule is given by eq 24.

On the basis of the temperature dependencies of the relaxation times $T_1(90 \text{ MHz})$ and $T_1(55.2 \text{ MHz})$ we determined the parameters of the methyl groups motions, Table 2, which could also be obtained from the NMR second moment measurements. Using the best-fit parameters obtained from $T_1(T)$ (Table 2), eq 24, and the structural data,³⁰ we calculated the theoretical dependence $M_2(T)$, see the solid line in Figure 5. The first two reductions (because of two dynamically inequivalent tunneling CH₃ groups) of the second moment occur near 0 K. These two reductions change the value of M_2 from 31.7 G² to 14.1 G². Then this value is kept up to about 42 K. At this temperature the tunneling motion of the labeled II methyl group ceases ($C_p T_{\text{tun(II)}} = E_{(II)}^{ov}$). Above 42 K, the second moment value

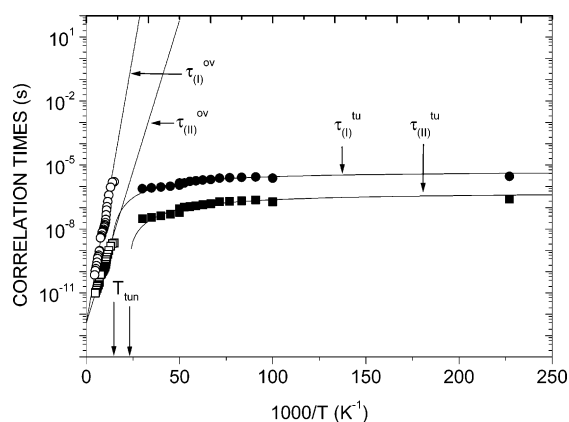


Figure 4. Proton correlation times $\tau_{(I)}^{ov}$ and $\tau_{(I)}^{tu}$ (circles) and $\tau_{(II)}^{ov}$ and $\tau_{(II)}^{tu}$ (squares) as a function of $1000/T$ [K⁻¹]. Points and lines refer to the experimental and theoretical correlation times, respectively. The motion parameters used in the calculations are taken from Table 2. Arrows show the temperatures $T_{\text{tun}(r)}$ (74 and 42 K).

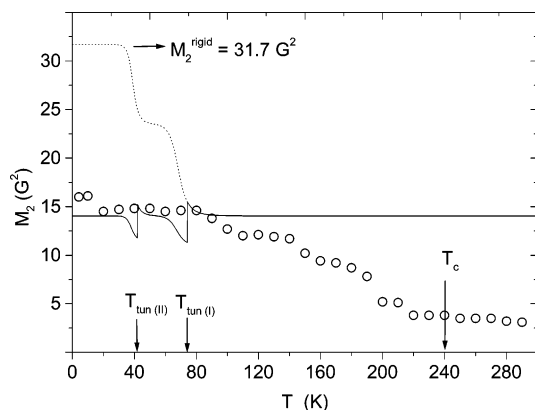


Figure 5. Points represent the experimental values of the second moment of the proton NMR of central line ω_1 for powdered samples of DMACA. The solid line is the theoretical plot obtained from eq 24 and the motion parameters from Table 2. The dotted line refers to the temperature dependence of M_2 obtained from eq 24 for $\tau_{(r)}^{tu} = \infty$. Arrows show the temperatures $T_{\text{tun}(r)}$ (74 and 42 K) and the temperature of the phase transition T_c (242 K).

should increase, but this effect is weak because the classical motion frequency ($1/\tau_{(II)}^{ov}$) starts to be comparable to the line width expressed on the frequency scale. The molecular frequency ($1/\tau_{(I)}^{tu}$) keeps the second moment at a reduced value up to about 74 K, where $C_p T_{\text{tun(I)}} = E_{(I)}^{ov}$. The subsequent reduction of the ω_1 line occurs when the rate of the classical motions ($1/\tau_{(I)}^{ov}$) becomes comparable with $\delta\nu$. The dashed line in Figure 5 shows the temperature dependence of M_2 due to the classical motion of two dynamically inequivalent methyl groups with the tunneling motion neglected.

The experimental data in Figure 5 show that above 150 K there are further reductions of the second moment. These reductions can be related to additional classical motions of the molecule. It can be the C_3 rotation of three DMA cations around their symmetry axis or quasi-isotropic motion of molecules in temperatures lower than that of the phase transition ($T_c = 242 \text{ K}$). To analyze the activation parameters of this motion we need to apply a formula for the spectral density of the complex motion of the vector R_{is} , including the two classical rotations.^{39,40,42,43} The analysis of the other types of motion in DMACA at the range of the high temperatures regime has been made in refs 35 and 36.

5. Conclusions

Proton spin–lattice relaxation T_1 and the proton second moment of the NMR line for [(CH₃)₂NH₂]₃Sb₂Cl₉ (DMACA) are affected by the classical C_3 rotation as well as incoherent tunneling of two dynamically different methyl groups belonging to the [(CH₃)₂NH₂⁺] cation.

1. The course of the proton $T_1(T)$ (55.2 MHz) dependence is mainly affected by the contribution of T_{1AE} .

2. The classical motion characterized by the correlation time $\tau_{(r)}^{ov}$ dominates at the highest temperatures, and the tunneling motion characterized by $\tau_{(r)}^{tu}$ dominates at the lowest temperatures.

3. The specific character of T_{1AE} in the range of intermediate temperatures ($20 \text{ K}^{-1} < 1000/T < 60 \text{ K}^{-1}$) refers to the significant shortening of the correlation time $\tau_{(r)}^{tu}$ below the temperature $T_{\text{tun}(r)}$ where the tunneling motion ceases.

4. The motion parameters obtained from the T_1 experiment, used for the calculation of the proton M_2 temperature dependence, explain well the narrowing of the NMR line at liquid helium temperatures. This narrowing is caused by the tunneling motion. Then the narrow line starts to be broadened in temperature regimes after cessation of the tunneling motion and before the narrowing caused by the classical motion. This should happen twice in the temperature scale for the reason of two dynamically inequivalent methyl groups.

Acknowledgment. This work was supported partially by the Polish State Committee for Scientific Research (project register 3TO9A 02326).

References and Notes

- (1) Gutowsky, H. S.; Pake G. E. *J. Chem. Phys.* **1950**, *18*, 162.
- (2) Andrew E. R. *J. Chem. Phys.* **1950**, *18*, 607.
- (3) Powles, J. G.; Gutowsky, H. S. *J. Chem. Phys.* **1953**, *21*, 1695.
- (4) Powles, J. G.; Gutowsky, H. S. *J. Chem. Phys.* **1955**, *23*, 1692.
- (5) Stejskal, E. O.; Gutowsky, H. S. *J. Chem. Phys.* **1957**, *28*, 388.

- (6) Stejskal, E. O.; Woessner D. E.; Farrar T. C.; Gutowsky, H. S. *J. Chem. Phys.* **1959**, *31*, 55.
- (7) Horsewill, A. J. *Prog. NMR Spectrosc.* **1999**, *35*, 359.
- (8) Köksal, F.; Rössler, E. *Solid State Commun.* **1982**, *44*, 233.
- (9) Köksal, F.; Rössler, E.; Sillescu, H. *J. Phys.: Solid State* **1982**, *15*, 5821.
- (10) Müller-Warmuth, W.; Schüler, R.; Prager, M.; Kollmar, A. *J. Chem. Phys.* **1978**, *69*, 2382.
- (11) Müller-Warmuth, W.; Schüler, R.; Prager, M.; Kollmar, A. *J. Magn. Reson.* **1979**, *34*, 83.
- (12) Montjoie, A.-S.; Müller-Warmuth, W. *Z. Naturforsch.* **1985**, *40a*, 596.
- (13) Haupt, J. *Z. Naturforsch.* **1971**, *26a*, 1578.
- (14) Johnson, Ch. S., Jr. *J. Magn. Reson.* **1976**, *24*, 63.
- (15) Johnson, Ch. S., Jr.; Wei, I. Y. *Chem. Phys. Lett.* **1975**, *35*, 236.
- (16) Hubbard, P. S.; Johnson, Ch. S., Jr. *J. Chem. Phys.* **1975**, *63*, 4933.
- (17) Andrew, E. R.; Eades, R. G.; Elsaffar, Z. M.; Llewellyn, J. P. *Bull. Amp.* **1960**, *9*, 379.
- (18) Eades, R. G.; Jones, G. P.; Llewellyn, J. P. *Proc. Phys. Soc.* **1967**, *91*, 632.
- (19) Eades, R. G.; Jones, G. P.; Llewellyn, J. P.; Terry, K. W. *Proc. Phys. Soc.* **1967**, *91*, 124.
- (20) Allen, P. S. *J. Chem. Phys.* **1968**, *48*, 3031.
- (21) Reynhardt, E. C.; Latanowicz, L. *J. Magn. Reson.* **1998**, *130*, 195.
- (22) Hennel, J. W.; Klinowski, J. *Fundamentals of Nuclear Magnetic Resonance*; Longman Scientific & Technical: Essex, England, 1993.
- (23) O'Reilly, D. E.; Tsang, T. *Phys. Rev.* **1967**, *157*, 417.
- (24) Latanowicz, L.; Reynhardt, E. C. *Chem. Phys. Lett.* **2001**, *341*, 561.
- (25) Latanowicz, L.; Reynhardt, E. C.; Boguszyńska, J. *J. Mol. Struct. (Theochem)* **2004**, *710*, 111.
- (26) Latanowicz, L. *J. Phys. Chem. A* **2004**, *108*, 11172.
- (27) Zaleski, J.; Pietraszko, A. *Acta Crystallogr.* **1996**, *B52*, 287.
- (28) Miniewicz, A.; Jakubas, R. *Solid State Commun.* **1987**, *63*, 933.
- (29) Jakubas, R. *Solid State Commun.* **1986**, *60*, 389.
- (30) Zalewski, J.; Pietraszko, A. *Acta Crystallogr.* **1996**, *B 52*, 287.
- (31) Mroz, B.; Andrews, T.; Clouter, M. J.; Jakubas, R. *J. Phys.: Condens. Matter* **1999**, *11*, 905.
- (32) Miniewicz, A.; Lefebrve, J.; Jakubas, R. *Ferroelectrics* **1990**, *107*, 183.
- (33) Jakubas, R.; Malarski, Z.; Sobczyk, L. *Ferroelectrics* **1988**, *80*, 193.
- (34) Idziak, S.; Jakubas, R. *Ferroelectrics* **1988**, *80*, 75.
- (35) Jagadeesh, B.; Rajan, P. K.; Venu, K.; Sastry, V. S. S. *Solid State Commun.* **1994**, *91*, 843.
- (36) Medycki, W.; Piślewski, N.; Jakubas, R. *Ferroelectrics* **1996**, *185*, 205.
- (37) Wichman, E. H.; *Quantum Physics*, Berkeley Physics Course; McGraw-Hill Book Company: New York, 1971. Vol. 4.
- (38) Bloembergen, N.; Purcell, E. M.; Pound, R. V. *Phys. Rev.* **1948**, *73*, 679.
- (39) Woessner, D. E. *J. Chem. Phys.* **1962**, *36*, 1.
- (40) Latanowicz, L.; Reynhardt, E. C. *Mol. Phys.* **1997**, *90*, 107.
- (41) Van Vleck, J. H. *Phys. Rev.* **1948**, *74*, 1168.
- (42) Latanowicz, L.; Andrew, E. R.; Reynhardt, E. C. *J. Magn. Reson.* **1994**, *A107*, 194.
- (43) Latanowicz, L.; Reynhardt, E. C. *J. Magn. Reson.* **1996**, *A121*, 23.
- (44) Powles J. G.; Mansfield P. *Phys. Lett.* **1962**, *2*, 58.
- (45) Powles J. G.; Strange J. H. *Proc. Phys. Soc.* **1963**, *82*, 6.
- (46) Mansfield P. *Phys. Rev.* **1965**, *137*, a961.
- (47) Van Cleemput, M.; Buekenhoudt, A.; Van Gerven, L.; Horsewill, A. J. *J. Chem. Phys.* **1995**, *103*, 2787.